

Article

Utilization of a Commercial 3D Printer for the Construction of a Bio-Hybrid Device Based on Bioink and Adult Human Mesenchymal Cells

Giulio Morelli ¹, Teresa Pescara ², Alessia Greco ², Pia Montanucci ², Giuseppe Basta ², Federico Rossi ¹ ,
Riccardo Calafiore ² and Alberto Maria Gambelli ^{1,*} 

¹ Engineering Department, University of Perugia, Via G. Duranti 93, 06125 Perugia, Italy

² Section of Internal Medicine and Endocrine and Metabolic Sciences (MISEM), Laboratory for Endocrine Cell Transplants and Biohybrid Organs, Department of Medicine, School of Medicine and Surgery, University of Perugia, Piazzale Gambuli, 06132 Perugia, Italy

* Correspondence: albertomaria.gambelli@unipg.it

Abstract: The biofabrication of three-dimensional scaffolds using 3D printers and cell-containing bioinks is very promising. A wide range of materials and bioink compositions are being created and tested for cell viability and printability in order to satisfy the requirements of a bioink. This methodology has not still achieved technological maturity, and the actual costs mean that they are often inaccessible for researchers, consequently lowering the development and extending the required times. This research aims to apply this methodology on a laboratory scale by re-adapting a commercial 3D printer, consequently lowering the costs and energy impacts, and, at the same time, ensuring a level of accuracy extremely close to the currently adopted devices and, more in general, suitable for the scopes of the research. To accomplish this, we assembled a biomimetic scaffold made of human Umbilical Cord Matrix Stem Cells (hUCMS), cellulose, and alginate. Various molds were used to produce 3D scaffolds of different sizes. After bioprinting, cell viability was analyzed using ethidium bromide and fluorescein diacetate, and a histological stain was used to evaluate cell and bioink morphology. All of the examined bioinks had a uniform final 3D structure and were stable, easily printable, and procedure-adapted. Up until 21 days of culture, the bioinks remained unaltered and were simple to manipulate. After 7 and 21 days of cell culture, the hUCMS in the cellulose/alginate-based bioinks exhibited cell viabilities of 95% and 85%, respectively. The cells did not present with a fibroblast-like shape but appeared to be round-shaped and homogeneously distributed in the 3D structure. Biomimetic bioink, which is based on cellulose and alginate, is an appropriate hydrogel for 3D bioprinting. This preliminary work illustrated the potential use of these two biomaterials for the 3D bioprinting of mesenchymal stem cells.

Keywords: 3D printer; cost and energy savings; printing setup; human mesenchymal stem cells; biomaterials; cellulose; alginate



Citation: Morelli, G.; Pescara, T.; Greco, A.; Montanucci, P.; Basta, G.; Rossi, F.; Calafiore, R.; Gambelli, A.M. Utilization of a Commercial 3D Printer for the Construction of a Bio-Hybrid Device Based on Bioink and Adult Human Mesenchymal Cells. *Energies* **2023**, *16*, 374. <https://doi.org/10.3390/en16010374>

Academic Editor: Dong Chen

Received: 11 October 2022

Revised: 9 December 2022

Accepted: 24 December 2022

Published: 29 December 2022



Copyright: © 2022 by the authors. Licensee MDPI, Basel, Switzerland. This article is an open access article distributed under the terms and conditions of the Creative Commons Attribution (CC BY) license (<https://creativecommons.org/licenses/by/4.0/>).

1. Introduction

The term 3D printing commonly refers to a group of different technologies, among them: additive manufacturing (AM), rapid prototyping (RP), layered manufacturing (LM), and solid free-form fabrication (SFF) [1]. It consists of automated and highly flexible technology, which is capable of producing complex 3D objects quickly and accurately based on a computer model [2]. These advantageous properties allow for reduced energy demand for the production of an object and also reduce the associated consumption of raw materials. For that reason, the usage of 3D printing techniques is assuming a key role in numerous sectors, such as transport, the medical sector, and the production of energy [3,4].

Depending on the typology of the working mechanism and the raw materials, different typologies of 3D bioprinting can be distinguished: inkjet-based, laser-based, and extrusion-

based [5]. Inkjet printing was the first technology implemented; it was carried out for the first time in the 1970s by the Hewlett-Packard company [6]. It consists of a non-contact image resolution technique. The presence of piezoelectric and thermal conductive nozzles allows for the generation of the pressure needed for the extrusion of bioink as droplets from the nozzle [7]. To apply such a technique, the raw materials should be liquid and should have a low viscosity [8]. Among the main advantages of it are the velocity of printing, the relatively low cost, and the maturity of the technology, which are probably the most meaningful [9].

Laser-based 3D printing is based on the pulsed energy of a laser, which allows for the control of the local pressure and causes the deposition of bioink [10]. The raw material consists of a cell-laden hydrogel within a polymer solution placed immediately below the laser-absorbing layer. The pulsed laser generates a vapour bubble on the receiving substrate and, due to this, applies the required pressure to deposit the bioink [11]. The main advantages of such a technique are the high precision and the absence of mechanical stresses [12].

Finally, extrusion-based printing dispenses bioink due to the action of mechanical and pneumatic systems [13]. The continuous application of air pressure produces an uninterrupted cylindrical filament [14,15]. Extrusion-based printing is probably the most applied technique because it ensures high versatility [16] and can work with several different typologies of bioink [17]. However, the accuracy of such a technique is the lowest when compared to the two previous solutions [18].

An important element of 3D printing is bioink, which must be suitable for in situ gelation, printability, shear thinning, and so on [19,20]. This material should ensure the production of a stable and high-resolution structure, and, at the same time, it should not affect cell viability during the printing process [21].

Bioprinting is a potential strategy to engineer 3D constructs with precisely defined structures and geometries by using living cells and biomaterials. Bioinks are a mixture of different biomaterials (such as hydrogels) and desired cell types to create functional tissue constructs, which are useful for replacing damaged or unhealthy tissues.

Bioinks can be cross-linked or stabilized during or right after printing to generate the final shape, structure, and architecture of the designed construct [22]. For printed tissues and organs to work properly, an ideal bioink must have the adequate mechanical, rheological, and biological properties of the target tissues [23].

Probably the most limiting factor to the extension of the experimental research in this field is the fact that, in recent years, extrusion-based bioprinting systems have been characterized by high development costs. Reducing these costs would extend the group of researchers involved in this field and, consequently, accelerate the achievement of the key targets fixed for the forthcoming years. In addition, the technological development of 3D bioprinters will also lead to reducing the energy required for the production of these devices and the emissions associated with the whole production chain. To circumvent the high-price barrier to the entry of conventional bioprinters, in the present work, the engineering of a low-cost and commercially available 3D printer has been carried out.

We wanted to use this type of printer to produce a new regenerative biomimetic hUCMS/cellulose-based scaffold. This scaffold should be comprised of human Umbilical Cord Matrix Stem Cells (hUCMS), cellulose, and alginate. Stem cells are a special type of cell population distinguished by their capacity for self-renewal and cellular differentiation. They are a desirable candidate for tissue regeneration due to these qualities. Specifically, adult stem cells, known as hUCMS (human umbilical cord Wharton jelly-derived mesenchymal stem cells), are deemed to be capable of differentiating, both in vitro and in vivo, into a variety of cell phenotypes [24–26]. The expression of chemokine and adhesion molecule receptors is probably connected to hUCMS homing tendencies [27]. The finding that hUCMS are immunoprivileged because they lack HLA-DR class II while also being linked to immunomodulatory features has stoked additional therapeutic interest [28–30]. These characteristics appear to be related to the humoral factors (IDO, iNOS, IL-6, PGE2,

TGF-1, HGF, VEGF) released from hUCMS, as well as their interactions with the target cells [31–34]. Additionally, the HLA-E, HLA-F, and HLA-G families are all expressed by hUCMS. These molecules are important in the fetal–maternal interface’s tolerogenic process [35]. In particular, it has been noted that the expansion of Treg cells is facilitated by the release of HLA-G from human mesenchymal stem cells [36]. Type 1 diabetic mellitus (T1D) and Sjogren syndrome (SSJ) are two autoimmune diseases where we have recently demonstrated the immuno-regulatory capabilities of hUCMS [30,37].

Although a biomimetic scaffold consisting of hUCMS and cellulose is simple to create, various problems of a technical nature have emerged during the manual preparation of the construct. In fact, the manual constitution results are operator-dependent and do not allow optimal standardization. In our opinion, all of these problems can be solved through 3D printing.

In this study, we focused on the implementation of a commercial 3D printer for the deposition of a biomimetic scaffold containing two biomaterials (cellulose and alginate) in combination with adult human mesenchymal stem cells (hUCMS). The printed bioink should allow for the uniform distribution of cells and interconnectivity with the external environment; it must also be stable and easily manipulated for use in regenerative medicine procedures.

2. Materials and Methods

2.1. Experimental Apparatus

2.1.1. 3D Printer

The chosen printer is a Cartesian 3D printer named 3DRAG, made by the Italian company Futura Elettronica, built of extruded aluminium profiles designed for interlocking or bolted fastening. The print bed can move along the X/Y axes, while the movement along the Z axis is exclusive to the extruder support bar. 3DRAG is also based on software compatible with the RepRap project; it can, therefore, benefit from a vast array of software and hardware that are natively compatible or easily adaptable. The limited dimensions of the machine (L: 50 cm, D: 42 cm, H: 62 cm, weight: 9 kg) easily allowed us to start and develop the printing process under sterile conditions within a controlled aspiration system (laminar flow hood) (Figure 1).

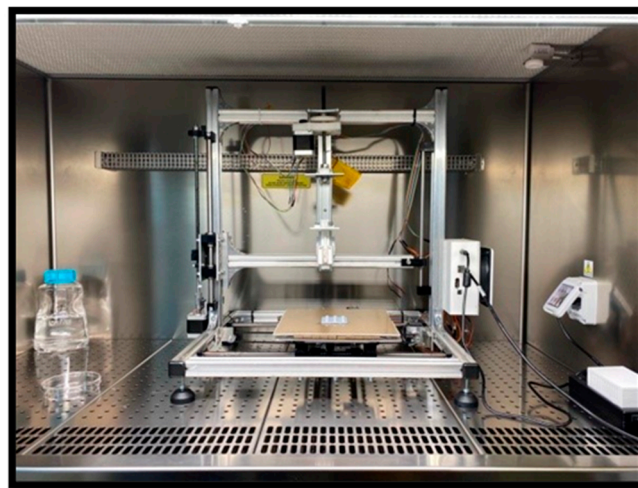


Figure 1. The 3DRAG 3D printer in the safety hood.

Repetier software was used to manage the printer, which is produced by Hot-World GmbH & Co. KG. Repetier is one of the most used software for 3D printing using common RepRap printers. Moreover, its practical graphic interface allows for the easy management of both the print bed by positioning and scaling objects before giving the Slicing command to generate the G-code; the printer allows for the performance of manual movements and

actions (for example, activating the heating of the extruders or varying the fan speed for cooling down). Another interesting function is “printing without extrusion” or “debug”, which are useful for checking if the printer is able to perform the desired movements.

2.1.2. Supplementary Devices

The experimental setup was completed with the following supplementary devices:

- A safety hood for biological hazards, with a working area protected by vertical laminar flow classified class II-Type A/B3, HEPA filter (model 120 standard, Bio Activa, AQUARIA). This device was purchased from GENELAB SRL, Perugia (Italy).
- Biological laboratory refrigerator KW class KLAB HTS MEDICAL PROJECT series (model KLAB-R1500V-HTS). Equipped with tropicalised refrigeration system, capable of working in critical environmental conditions and GMP-compliant internal ventilated refrigeration. Working temperature from 0 °C to +15 °C. This device was purchased from GENELAB SRL, Perugia (Italy).
- Incubator (Thermo Electron Model 371 Steri Cycle CO₂ Incubator) maintains the desired conditions, including temperature (37 °C), humidified air (95%), and CO₂ concentration (5%). This direct-heat incubator features an in-chamber HEPA air filtration system. This device was purchased from GENELAB SRL, Perugia (Italy).

2.2. Materials

2.2.1. Inks Preparation

The composition of the bioink is based on the protocol proposed by Markstedt et al. with some modifications [38].

The printing trials involved the use of bioink1, consisting of alginate, mannitol, and microfibrillar cellulose (MFC) in different concentrations, and bioink2, consisting of alginate, mannitol, and nanocrystalline cellulose (CNC).

Alginic acid is a polysaccharide extracted from the cell walls of brown seaweeds (*Phaeophyceae*). Alginates are linear copolymers made of two building components, β -D-mannuronic (M) and α -L-guluronic (G) acids, which are primarily arranged in the form of MM or GG or MG dimeric blocks across the entire molecule. Alginates are used as thickeners and stabilizers in the food, pharmaceutical, and cosmetics industries. The powdered alginate (AG) was purchased from Monsanto-Kelco (San Diego, CA, USA) and was characterized by the following properties: molecular weight = 120,000–190,000 kDa; main AG polymers: mannuronic acid (M) and guluronic acid (G) patterned as following; M fraction (FM) 61%; G fraction (FG) 39%. It is a “high-M” alginate. It was dissolved in 4.6% (*v/v*) D-mannitol saline solution (Fresenius Kabi, Bad Homburg, Germany) at a concentration of 2.5% (*w/v*). D-mannitol was used to retain the osmolarity (Published online 13 March 2014. <https://doi.org/10.1371/journal.pone.0091662>).

For our studies, we used two types of cellulose: microfibrillar F cellulose (MFC) (EXILVA F 01-V, Borregaard, Sarpsborg, Norway) and Cellulose NanoCrystalline (CNC) (CelluForce NCC[®] NCV-100) (Figure 2).

Exilva F 01-V is a microfibrillated cellulose that is entirely natural, biodegradable, and multifunctional. The typical areas of use for the Exilva F series are mainly the manufacture of personal care products, home care, agricultural chemicals, paints, and adhesives. It is non-toxic, anti-blocking, and odorless. It is available as a 2% suspension or a 10% paste. It enhances the rheology and stability of water-based paints as well as premium industrial and architectural paints and coatings. It demonstrates strong compatibility with salts, surfactants, and polar solvents. It creates a network of non-soluble fibers that resembles a polymer. It increases film strength and has good water resistance, adhesion, and reinforcement. It also offers greater durability.



Figure 2. Cellulose used for this study: microfibrillar F cellulose (MFC) EXILVA and CelluForce[®] nanocrystalline cellulose (CNC).

CelluForce NCC[®] is a natural product that is safe, biodegradable, and multifunctional. It can be economically extracted from wood fibers and is an abundant and renewable resource. CNC is prepared as a spray-dried powder or as a liquid suspension and can be utilized to enhance product performance in a variety of industrial sectors. CNC is made of infinitely tiny cellulose crystals generated from trees.

Nanocrystalline cellulose consists of crystals that can interact with each other based on their size, charge, and shape. The crystals have high stiffness and tensile strength, comparable to hard metals and their alloys. However, they are nano-sized and are not strongly interconnected except in the structures established by nature from which they are isolated or when aggregated or incorporated into matrices and films.

The ink was prepared by dissolving alginate in a saline solution of mannitol; then, the cellulose was incorporated and mixed using a homogenizer (Omni GLH850 General Laboratory Homogenizer, PerkinElmer, Inc., Waltham, MA, USA). The preparation was steam sterilized in an autoclave (121 °C for 10') and cooled to room temperature. Four formulations of bioinks were prepared with different concentrations of cellulose, as seen in Table 1. All of the bioink formulations were stored at 4 °C under sterile conditions.

Table 1. Ink formulations using various cellulose concentration.

	Alginate (<i>w/v</i>)	Mannitol Saline Solution (<i>v/v</i>)	NanoCrystalline Cellulose (CNC) (CelluForce NCC [®])	Microfibrillar Cellulose F (MFC) EXILVA	Viscosity [mPa s]
<i>Bioink1</i>	2.5%	4.6%		2.5%	806,936 ± 12,404
	2.5%	4.6%		1.5%	319,124 ± 4149
	2.5%	4.6%		0.5%	55,072 ± 881
<i>Bioink2</i>	2.5%	4.6%	2.5%		16,344 ± 327

2.2.2. hUCMS Isolation and Cell Culture Maintenance

hUCMS were isolated from postpartum human umbilical cords, as described by Montanucci et al. [24]. The recovered cells were seeded at a concentration of 6000–8000/cm² per treated flask in a CMRL Medium 1066 1X (Gibco, Invitrogen, Waltham, MA, USA) supplemented with 10% Fetal Bovine Serum (FBS, Euroclone, Pero, Italy), 1X L-glutamine (Gibco), 1X penicillin/streptomycin (Gibco) (normal medium, NM). The hUCMS were maintained at 37 °C under 5% CO₂ in humidified 95% air. Then, 80% of the confluent cells were treated with 0.05% trypsin/EDTA (Gibco) for 3 min at 37 °C, and, subsequently, the serum was added to stop the trypsin activity. The bioinks were created using cells at III-IV culture passage.

2.3. Experimental Procedure

2.3.1. Modifications Applied to the 3D-Printer for the Scope

The original printer mainboard was replaced with a Megatronics v3.3 (datasheet [megatronicsv33.pdf](#) ([reprapworld.it](#))) because of the upgraded computing power and the capability to manage improved stepper motors drivers. The drivers were replaced, going from the original model (Pololu A4988) to an improved model named DRV8825 to take advantage of the improved heat dissipation and the greater microstepping allowed by the later model.

Additionally, to reduce the manipulations of the bioink, scaffold, and supports, and to avoid external contaminations and speed up the printing process, the sequential printing protocol was implemented in the firmware, allowing us to easily print up to 9 copies of the same device in a single row.

To proceed with the deposition of the bioink, the system used in the course of this work is based on the one that already equipped the 3DRAG printer, resulting in the modification of a rather peculiar accessory of the 3DRAG, which is suitable for the deposition of melted chocolate through the process of 3D printing. This accessory consists of a syringe holder and a piston moved by a threaded rod, a nut, and a cogwheel to couple the system with another NEMA 17 stepper motor. The extruder was modified in the end part; we decided to use common syringes with a capacity of 3 mL, Luer-lock, with 22G 0.625'' tip needles, as they are easy to find, cheap, and easily adaptable for this purpose. To hold the syringe in place, a syringe holder made of two main parts to allow for easy adjustments, was built (with PLA) with another 3D printer (Figure 3).

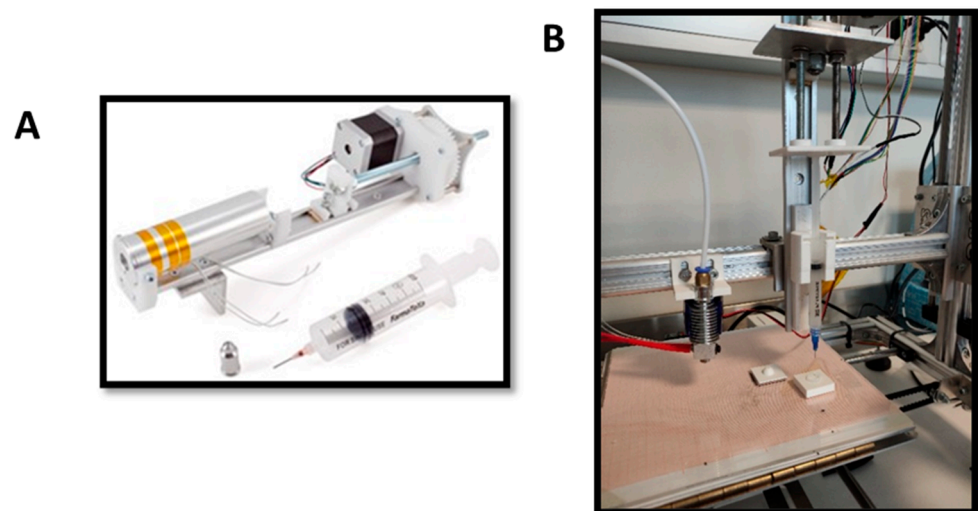


Figure 3. (A) The original extruder and (B) the modified version (RIGHT), assembled on the extruder beam of the 3DRAG next to the polymer extruder (LEFT).

2.3.2. Printer Tuning and Printing Method

Before being able to proceed with the extrusion of the bioink, it was necessary to analyze how it can interact with the extrusion system itself. In particular, it is fundamental to understand the behavior of the bioink once subjected to the pressure of the piston; in fact, the viscosity and the shear-thinning behavior influenced the choice of the extrusion speed, the printing movement speed, and the pressure that the syringe piston must exert on the ink. The rate of descent of the piston is not a parameter that can be modified directly from the interface of the printer management program, as it is linked to the number of revolutions (step/mm) of the extruder electric motor.

The first calibration of the printer was carried out to adapt it to the new configuration of the extruder: the lower limit switch of the Z axis was repositioned and then adjusted in order to have the nozzle of the syringe at the correct height with respect to the printing

surface. After verifying the correct movements of the printer on all the axes, the first deposition test of the bioink was carried out. For the first series of prints, bioink1 was used, which is made up of alginate and microfibrillar cellulose, 2.5% and 1.5%, without cell components because the prints would not have been made in an aseptic environment (Figure 4).

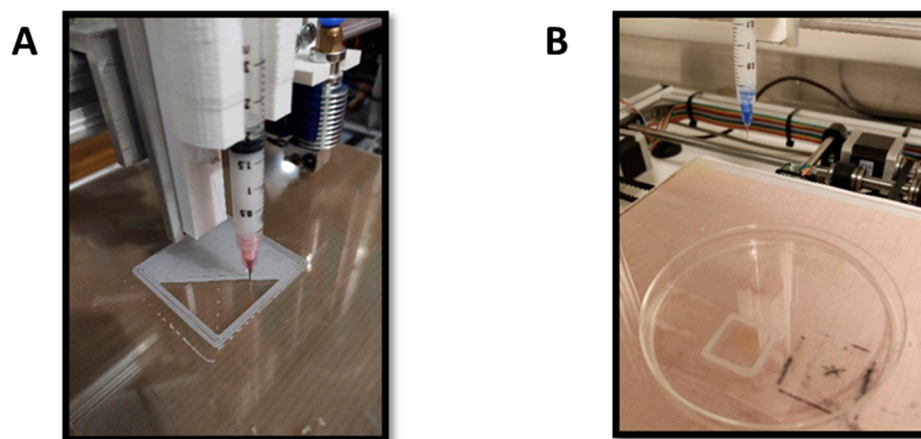


Figure 4. (A) First deposition test, directly over the PVC bed and (B) One of the squares printed, into a Petri plate, 20 mm side.

From the first rounds of depositions, it quickly emerged that the 3DRAG, excluding some small and necessary refinements, enjoys good control over the amount of bioink extruded and on the geometry of the figures; in fact, it is possible to print the desired geometries with good reliability and repeatability.

2.3.3. Definition of the Shapes Selected for Printing

The shapes to be printed were selected both on the basis of the printability criteria using the available equipment and the functional criteria. In the beginning, mostly to calibrate the printer movements, simple shapes such as circumferences, circles, and squares made of only one or two layers were printed.

After ensuring the printability and repeatability of the shapes (Table 2), we decided to print a semi-spherical shape with a 9 mm diameter, which was printed dome-like on a support made with PLA; this choice was taken to have a shape that could be relatable to other shapes used in microbiology, the shape was reminiscent of the microcapsules commonly used to enclose solids, liquids, or gases inside a micrometric wall made of hard or soft soluble films, in order to reduce dosing frequency and prevent the degradation of pharmaceuticals [39]. Additionally, the hollow semi-sphere, made with a tougher bioink (bioink1), can be overturned and filled with the less viscous (and softer) bioink, bioink2. To ascertain this, the viscosity of both bioinks was measured with a viscosimeter, model ViscoStar Plus R. The viscosity was measured in “mPa s” and is shown in Table 1 (Section 2.2.1).

Table 2. Shapes selected and related sizes.

Shape	Nominal Size	Real Size
SQUARE	Side:10 mm	Side: 10.36 mm \pm 0.05 mm
SQUARE	Side: 20 mm	Side: 20.72 mm \pm 0.05 mm
CIRCUMFERENCE	Diameter: 10 mm	Diameter: 10.22 mm \pm 0.05 mm
CIRCUMFERENCE	Diameter: 20 mm	Diameter: 20 mm

Subsequently, a second and third series of prints were carried out in the laboratory for Endocrine Cell Transplantation and Biohybrid Organs of the department of Medicine

and Surgery of the University of Perugia. The 3DRAG was placed into the vertical flow hood in order to guarantee the sterility of the deposition process. To ensure the uniformity of the printing process, repeatability, the absence of contact with foreign bodies during the printing, and support for the bioink, some PLA-made printing bases were realized (Figure 5), the placement of the supports in a common multiwell capable of housing up to 6 supports (and consequently 6 hemispheres in bioink) allowed us to take advantage of the sequential printing protocol.

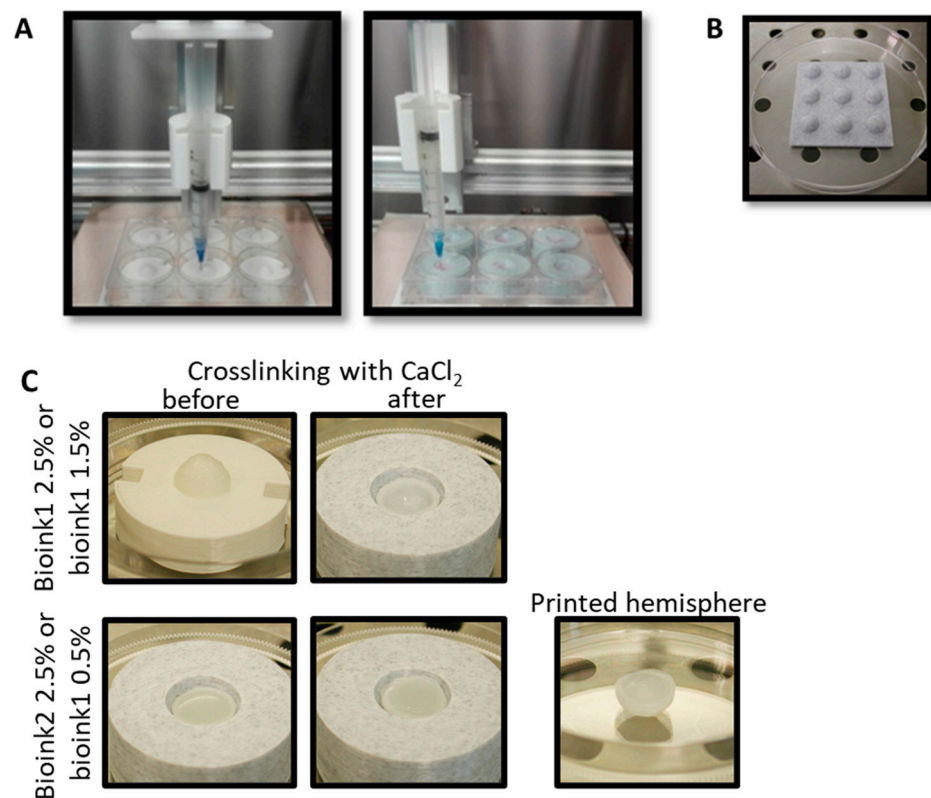


Figure 5. The deposition of the bioink in the biosafety cabinet. (A) on the left, the print of the hollow hemispheres (bioink1 2.5% or 1.5%) on white PLA molds with 9 mm diameter, (A) on the right, the print of bioink2 2.5% or bioink1 0.5% inside the crosslinked hollow hemisphere on grey PLA molds. (B) Grey PLA molds with 7 mm diameter. (C) Printed bioinks before and after crosslinking with CaCl₂ and final 3D structure (hemisphere).

Serial printing was used to speed up the printing and shorten the time that the cells were left at room temperature. Additionally, different-sized molds (9 and 7 mm in diameter) were used to reduce the amount of print material needed (see Figure 5).

The chosen procedure involved the making of six hollow hemispheres on the (A) base, then, after a manual overturning, the printing of another hemisphere, flat side up, was used to fill the empty part of the bioink1-made sphere with bioink2.

A commercial 3D printing device was used for the deposition of the bioink and 9- and 7-mm-diameter molds that were used for serial printing.

2.3.4. Procedure Used for the Insertion of Cells-Bioprinting with hUCMS

hUCMS were mixed into the bioink at a final concentration of 10×10^6 cells/mL. The bioink was transferred into the Luer-Lock syringe using a sterile spatula or a micropipette, and then the syringe was placed in the syringe holder.

After printing, the constructs were cross-linked in 90 mM CaCl₂ solution for 10 min and rinsed twice in saline solution. The 3D culture was maintained under standard conditions (37 °C, 5% CO₂ and humidified 95% air). Then, a normal medium was added to the bioink

and was changed every three days. The cell-filled 3D bioprinted constructs were evaluated after being maintained overnight (O/N) on the 7th, 14th, and 21st days of culture.

2.3.5. Evaluation of the Printed Shapes

Structurally, the bioink remains intact and can be easily manipulated for the entire duration of the culture phase; the viscous consistency of the bioink1 allowed us to print shapes with up to a 9 mm diameter without observing major sagging or deviations from the nominal shape or size of the bioink-made device.

2.3.6. Evaluation of Cells' Vitality—Viability Assay

During the phase culture, the cell viability assay was performed at different time points to verify the survival of the cells across several culture days. The samples were washed in a saline solution and then incubated in the staining solution. A mixture containing Ethidium Bromide $1\times$ (0.2 mg/mL) in PBS $1\times$ was prepared to highlight the dead cells in red, and Fluorescein Diacetate in acetone (5 mg/mL) to verify the presence of live cells (that appeared in green).

2.3.7. Morphological Evaluation

The printed bioinks were evaluated morphologically using phase contrast microscopy using a Nikon TS100 microscope.

2.3.8. Histological Analyses: Sample Preparation and Specific Staining

The bioinks made by the 3D printer were evaluated morphologically by histological staining with hematoxylin/eosin. At different time points, the bioinks were fixed in 10% neutral buffered formalin for 30 min at room temperature and subsequently dehydrated and paraffin-embedded. Using a rotary microtome, the paraffin-embedded specimens were cut into 4- μ m-thick slices and stained in accordance with standard histological protocols. The bioinks were observed with phase-contrast microscopy using a Nikon Eclipse Ci microscope.

3. Results

3.1. Deposition Procedure and Valuations over the Shapes

The first series of prints consisted of the printing of simple figures, such as squares and circumferences, using bioink1 2.5% MFC due to its higher viscosity and resistance to handling, which makes it more printable than the compounds with a lower cellulose content. Furthermore, the loading of the syringe (3 mL) with bioink1 was found to be very simple, using a small spatula and making sure not to leave any air bubbles.

Having ensured the good quality and repeatability of the prints, printing squares, circumferences, and domes with both bioink1 2.5% and 1.5% MFC, without the cell fraction, we performed a second series of prints; in the second series, the main objective was to print with the cell fraction, domes with bioink1 2.5% and 1.5% MFC and the semi-spheres with bioink2 2.5% CFC and bioink1 0.5% MFC.

To print the domes, it was necessary to create a smaller (10-mm diameter or less) dome-shaped PLA support; this was performed in order to provide support for the bioink before the polymerization, avoiding the collapse of the structure. Additionally, to avoid excessive manipulations and contamination, having enabled the sequential printing protocol, a second support capable of holding a maximum number of 9 domes was used.

The encouraging results from a qualitative and quantitative point of view led to the third series of prints in which, in an attempt to reduce the amount of bioink used while keeping the quality of what was printed high, we went to work on the STL file by reducing the thickness of the dome wall from 1 mm to 0.7 mm. This operation was also carried out with the aim of improving the transport of nutrients during the cultivation phase.

In Table 3, a brief recap of the shapes printed and their sizes can be seen (side for squares, diameter for circumferences, semi-spheres, and domes).

Table 3. Shapes printed, sizes and number of prints.

Bioink	Shape	Size	Number of Prints
bioink1 2.5% MFC	Square	10 mm	8
bioink1 2.5% MFC	Square	20 mm	10
bioink1 2.5% MFC	Circumference	10 mm	10
bioink1 1.5% MFC	Circumference	20 mm	8
bioink1 2.5% MFC	Dome	9 mm	20
bioink1 1.5% MFC	Dome	8 mm	15
bioink2 2.5% CFC	Semi-sphere	7 mm	8

3.2. Analysis on Biological Material

Characteristics of Bioinks

Before cross-linking, the bioinks showed a different consistency due to the inherent properties of the two different celluloses. MFC cellulose is a homogenous paste, and bioink1 appeared denser and fuller-bodied, whereas bioink2 was a semi-dense mixture that tended to be more liquid (CNC is a freeze-dried powder).

Therefore, bioink1 2.5% and 1.5%, which showed a fair consistency and could be loaded into the Luer-Lock syringe using a sterile spatula. In contrast, bioink2 was a semi-dense mixture and could be inserted into the syringe using the P1000 micropipette. Bioink1 0.5% had a consistency suitable for loading similar to that of bioink2 (using the micropipette P1000).

During printing, bioink1 2.5% and 1.5% did not show any noticeable sagging and deformation when printed, so these bioinks could be used to build the outer structure of the hemisphere. Bioink1 0.5% showed limited consistency similar to bioink2 2.5% and could be used to print the inner portion of the hemisphere.

After the printing process, a 90 mM CaCl₂ solution was sprayed with a nebulizer directly onto the bioinks without removing them from the mold in order to ensure the stability of the 3D structure during the cross-linking process.

All of the bioinks were stable, readily printed, procedure-adapted, and demonstrated a uniform 3D final structure after the cross-linking process.

Structurally, bioinks were remained intact and easily manipulated throughout the duration of the culture (21 days). The cells showed optimal viability (95%) up to about one week of culture, in the following weeks the viability decreases to 85% up to day 21 of culture (Figure 6). This is likely caused by the prolonged culture period, the bioinks' compact nature and the size of the 3D structure (hemispheres with a diameter of 9 and 7 mm). This last condition could influence the adequate transport of nutrients (and waste substances).

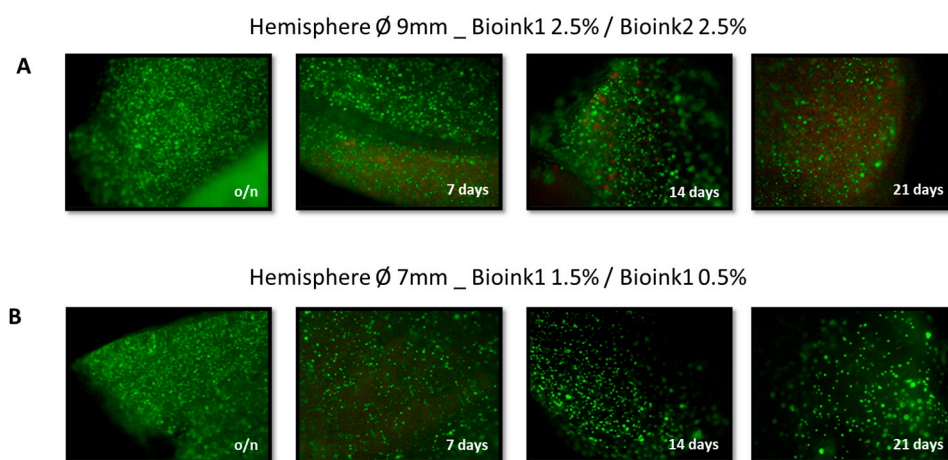


Figure 6. Evaluation of viability with fluorescein diacetate and ethidium bromide of bioink1 2.5%/bioink2 2.5% (A) and bioink1 1.5%/bioink1 0.5% (B) samples after O/N, 7, 14 and 21 days of culture (4× magnification).

During the culture period, the cells in the different bioink1 (2.5%, 1.5%, and 0.5%) and bioink2 2.5% did not show an elongated and fibroblast-like shape but appeared round-shaped, having no signs of distress and appearing to be homogeneously distributed.

Histological staining (haematoxylin/eosin) (H&E) on the printed bioinks was used to assess the cell morphology and structural differences between the bioinks (Figure 7). In contrast to bioink1, which appears homogeneous, compact, and devoid of “structures,” bioink2 seemed inhomogeneous and had “oval structures”.

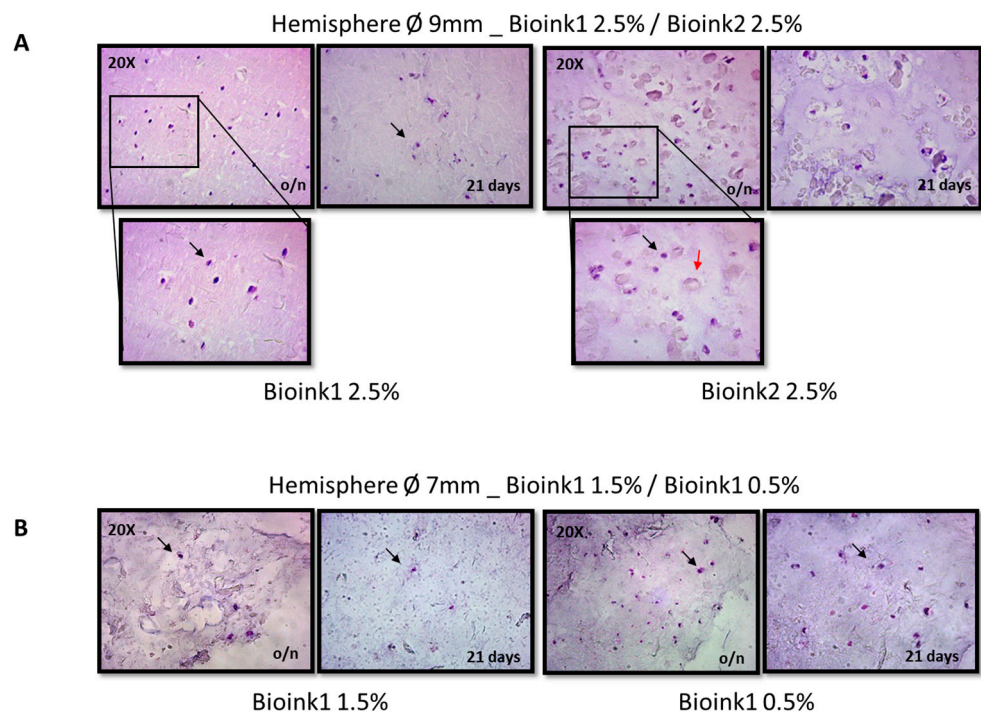


Figure 7. Representative histological staining (H&E) of the bioink1 2.5%/bioink2 2.5% (A) and bioink1 1.5%/bioink1 0.5% (B) samples. Black arrow indicates hUCMS. Red arrow indicates bioink2’s “oval structures” (20× and 40× magnifications).

4. Discussion

The objective of the work presented was to use a common commercial 3D printing device for bioprinting, adapting it with some limited hardware and software modifications, also testing the possibility of creating a bioink consisting of cellulose, alginate, and stem cells adult mesenchymal of the Wharton gel matrix (hUCMS), with the end last to use it to allow for the reparation and regeneration of damaged human tissues.

Essentially, the adaptation of the printer to the deposition of biological material required the modification of the extrusion system, so a holder able to house common medical injection syringes was designed and equipped with a direct current motor, which through a system gear and screw is capable of applying controlled pressure to the piston above the syringe, allowing the extrusion of the bioink.

The design and consequent implementation of the necessary hardware and software changes have therefore made it possible to print biological material through a common extrusion-based 3D printer.

The cost of the printer, including modifications made with common hardware-store components and mechanical tools, is at least twenty times lower when compared to commercial bioprinters with comparable techniques and mechanics. The results obtained, therefore, encourage the development of bioprinters with appreciable properties and print quality but with a relatively low spending target, when the focus is to allow for greater and more rapid diffusion of bioprinting in universities, medical schools and laboratories, allowing for the expansion of the research in the field.

The chosen cell model has recently attracted increasing interest due to the many advantages associated with its use. hUCMS are umbilical cord cells, which are disposed of after birth as medical waste and do not create ethical problems. An effective and repeatable enzymatic digestion procedure is used to separate these cells from the human umbilical cord, ensuring homogeneity in the cell phenotype [24].

The ability of hUCMS to differentiate *in vitro* and *in vivo* in tissues of mesodermal (cartilage, tendons, bones, ligaments, adipose tissue, connective tissue), ectodermal (neural cells), and endodermal (pancreatic progenitors) tissues is supported by the expression of both genetic and surface markers typical of mesenchymal cells (CD10, CD29, CD44, CD90, CD105), as well as markers typical of stemness (OCT4, SOX2, Nanog) [24,40,41].

Three-dimensional bioprinting has generated some interest due to the usage of natural resources from plants, algae, and microorganisms, such as cellulose, lignin, alginate, and chitosan. Alginate and cellulose were selected as the biomaterials in our study to create the scaffold (bioink).

Alginic acid is one of the main constituents of the cell wall of marine macroalgae (brown algae), is considered an FDA (Food and Drug Administration, Silver Spring, MD, USA) approved compound, and is used in numerous pharmaceutical preparations, e.g., for the treatment of symptoms related to gastro-oesophageal reflux and digestive difficulties. The most prevalent biopolymer found in plant cell walls is cellulose, which is very simple to combine with other substances. These polymers are preferable to synthetic materials due to their biocompatibility, biodegradability, and lower immunogenicity.

In our investigation, two different types of 3D scaffolds were realized by utilizing the ductility and properties of the above-mentioned biomaterials. In the first instance, a 3D scaffold made of hUCMS known as bioink1 2.5%/bioink2 2.5% was realized, the scaffold's outside (more compact) component was built of 2.5% MFC microfibrillar cellulose, and the interior of the 3D structure was made of 2.5% CNC nanocrystalline cellulose.

In the second instance, a 3D scaffold containing hUCMS was created and given the name bioink1 1.5%/bioink1 0.5%. It was made of 1.5% MFC microfibrillar cellulose for the scaffold's outside (more compact) component and 0.5% MFC microfibrillar cellulose for the interior of the 3D structure.

The scaffolds made with these bioinks delivered the best and most unchanged results in the cell viability testing (up to 21 days of culture). The cells showed no signs of distress, were viable and well distributed throughout the bioink. This is most likely caused by the ink's disorganized structure and the manner the cellulose crystals are arranged. Therefore, it can be claimed that this method of bioprinting is suitable for using hUCMS, cellulose, and alginate. Over the examined culture period of 21 days, bioink was stable and durable, suitable for printing, and moldable. The usefulness of nebulization, the simplicity of printing and handling, and the economic advantage are additionally acknowledged.

It can therefore be said that the developed extrusion technique is adequate for the type of bioink used, especially considering the ease of the modifications required for the printer, the simple manipulation of bioink and the equipment, as well as the cost-effectiveness of the solution created. The results obtained, based on the evaluation of the bioink-based scaffolds, encourage future studies that will include further *in vitro* and *in vivo* experiments.

The *in vitro* studies will be aimed at the characterization of hUCMS in the bioink and at the standardization of the scaffold realization methods through the deposition technology with a modified commercial 3D printer. The goal is to guarantee a better yield of the product, minimizing the numerous operator-related variables.

Instead, from a hardware point of view, future studies and further development will include the possibility of implementing a double extrusion system since the mainboard of the printer allows the control of up to six stepper motors; this means that with an additional extruder, it would be possible to dispense simultaneously or in sequence two different bioink solutions or even two different materials, such as for example PCL (polycaprolactone) which could be used to realize biocompatible supports for the bioink scaffolds.

5. Conclusions

The present research deals with the design and implementation of a commercial 3D printer for the deposition of biomimetic scaffolds containing two different types of biomaterials, respectively, alginate and cellulose, and in combination with adult human mesenchymal stem cells (hUCMS). Because this research and medical sector have not still reached technological maturity, the currently adopted devices are extremely expensive and do not take into account the energy costs and environmental impact of their utilization together with the whole supply chain. These criticisms (especially costs) make this technology unavailable for most researchers and, consequently, would lead to a significant delay in reaching technological maturity in the field.

If a commercial 3D printer can be adapted for the same scopes and its accuracy and overall performances are proved to be close to those of the previously cited devices, the research into the deposition of biomimetic scaffolds containing biomaterials and hUCMS could be widely extended and improved. This article aimed to provide the experimental validation of this latter thesis.

Biomaterial technology combined with human stem cells opens new possibilities for regenerative medicine. Therefore, the basis for regenerative medicine will be set by future research that can consider both stem cell biology and the chemical and mechanical properties of biomaterials. These studies will concentrate on the development of new microscale devices as well as the spatial distribution of molecules that define physicochemical stimulation and direct stem cells toward specific differentiation and tissue/organ reconstitution.

Author Contributions: Conceptualization, T.P. and A.G.; methodology, T.P., G.M. and A.G.; software, G.M. and A.M.G.; validation, G.B., P.M. and R.C.; formal analysis, T.P. and A.M.G.; investigation, A.G.; resources, F.R. and R.C.; data curation, G.M., T.P. and A.G.; writing—original draft preparation, G.M., T.P., A.G. and A.M.G.; writing—review and editing, T.P. and G.M.; visualization, P.M. and G.B.; supervision, R.C.; project administration, R.C.; funding acquisition, R.C. and F.R. All authors have read and agreed to the published version of the manuscript.

Funding: This research received no external funding.

Data Availability Statement: Not applicable.

Conflicts of Interest: The authors declare no conflict of interest.

References

1. Melchels, F.P.W.; Domingos, M.A.N.; Klein, T.J.; Malda, J.; Bartolo, P.J.; Huttmacher, D.W. Additive manufacturing of tissues and organs. *Prog. Polym. Sci.* **2021**, *37*, 1079–1104. [[CrossRef](#)]
2. Wang, X.; Yan, Y.; Zhang, R. Rapid prototyping as a tool for manufacturing bioartificial livers. *Trends Biotechnol.* **2007**, *25*, 505–513. [[CrossRef](#)] [[PubMed](#)]
3. Gambelli, A.M.; Stornelli, G.; Di Schino, A.; Rossi, F. Methane and carbon dioxide hydrates properties in presence of Inconel 718 particles: Analyses on its potential application in gas separation processes to perform efficiency improvement. *J. Environ. Chem. Eng.* **2021**, *9*, 106571. [[CrossRef](#)]
4. Gambelli, A.M.; Stornelli, G.; Di Schino, A.; Rossi, F. Methane and carbon dioxide hydrate formation and dissociation in presence of a pure quartz porous framework impregnated with CuSn12 metallic powder: An experimental report. *Materials* **2021**, *14*, 5115. [[CrossRef](#)] [[PubMed](#)]
5. Mahendiran, B.; Muthusamy, S.; Sampath, S.; Jaisankar, S.N.; Popat, K.C.; Selvakumar, R.; Krishnakumar, G.S. Recent trends in natural polysaccharide based bioinks for multiscale 3D printing in tissue regeneration: A review. *Int. J. Biol. Macromol.* **2021**, *183*, 564–588. [[CrossRef](#)] [[PubMed](#)]
6. Derakhshanfar, S.; Mbeleck, R.; Xu, K.; Zhang, X.; Zhong, W.; Xing, M. 3D bioprinting for biomedical devices and tissue engineering: A review of recent trends and advances. *Bioact. Mater.* **2018**, *3*, 144–156. [[CrossRef](#)]
7. Bose, S.; Vahabzadeh, S.; Bandyopadhyay, A. Bone tissue engineering using 3D printing. *Mater. Today* **2013**, *16*, 496–504. [[CrossRef](#)]
8. Yeong, W.; Chua, C.; Leong, K.; Chandrasekaran, M.; Lee, M. Indirect fabrication of collagen scaffold based on inkjet printing technique. *Rapid Prototyp. J.* **2006**, *12*, 229–237. [[CrossRef](#)]
9. Schuurman, W.; Levett, P.A.; Pot, M.W.; van Weeren, P.R.; Dhert, W.J.A.; Huttmacher, D.W.; Melchels, F.P.W.; Klein, T.J.; Malda, J. Gelatin-Methacrylamide hydrogels as potential biomaterials for fabrication of tissue-engineered cartilage constructs. *Macro-Mol. Biosci.* **2013**, *13*, 551–561. [[CrossRef](#)]

10. Dababneb, A.B.; Ozbolat, I.T. Bioprinting technology: A current state-of-the-art review. *J. Manuf. Sci. Eng.* **2014**, *136*, 061016. [[CrossRef](#)]
11. Thavornnyutikam, B.; Chantarapanich, N.; Sitthiseripratip, K.; Thouas, G.A.; Chen, Q. Bone tissue engineering scaffolding: Computer-aided scaffolding techniques. *Prog. Biomater.* **2014**, *3*, 61–102. [[CrossRef](#)]
12. Li, W.; Sun, W.; Zhang, Y.; Wei, W.; Ambasadhan, R.; Xia, P.; Talantova, M.; Lin, T.; Kim, J.; Wang, X.; et al. Rapid induction and long-term self-renewal of primitive neural precursors from human embryonic stem cells by small molecule inhibitors. *Proc. Natl. Acad. Sci. USA* **2011**, *108*, 8299–8304. [[CrossRef](#)]
13. Mouser, V.H.M.; Levato, R.; Bonassar, L.J.; Darryl, D.D.; Grande, D.A.; Klein, T.J.; Saris, D.B.F.; Zenobi-Wong, M.; Gawlitta, D.; Malda, J. Three-dimensional bioprinting and its potential in the field of articular cartilage regeneration. *Cartilage* **2017**, *8*, 327–340. [[CrossRef](#)]
14. Peltola, S.M.; Melchels, F.P.W.; Grijpma, D.W.; Kellomaki, M. A review of rapid prototyping techniques for tissue engineering purposes. *Ann. Med.* **2008**, *40*, 268–280. [[CrossRef](#)]
15. Panwar, A.; Tan, L.P. Current status of bioinks for micro-extrusion-based 3D bioprinting. *Molecules* **2016**, *21*, 685. [[CrossRef](#)]
16. Ozbolat, I.T.; Hospodiuk, M. Current advances and future perspectives in extrusion-based bioprinting. *Biomaterials* **2016**, *76*, 321–343. [[CrossRef](#)]
17. Hiller, T.; Berg, J.; Elomaa, L.; Rohrs, V.; Ullah, I.; Schaar, K.; Dietrich, A.C.; Al-Zeer, M.A.; Kurtz, A.; Hocke, A.C.; et al. Generation of a 3D liver model comprising human extracellular matrix in an alginate/gelatin-based bioink by extrusion bioprinting for infection and transduction studies. *Int. J. Mol. Sci.* **2018**, *19*, 3129. [[CrossRef](#)]
18. Jakab, K.; Norotte, C.; Damon, B.; Marga, F.; Neagu, A.; Besch-Williford, C.L.; Kachurin, A.; Church, K.H.; Park, H.; Minorov, V.; et al. Tissue engineering by self-assembly of cells printed into topologically defined structures. *Tissue Eng. Part A* **2008**, *14*, 413–421. [[CrossRef](#)]
19. Gu, B.K.; Choi, D.J.; Park, S.J.; Kim, Y.J.; Kim, C.H. 3D bioprinting technologies for tissue engineering applications. *Adv. Exp. Med. Biol.* **2018**, *1078*, 15–28.
20. Murphy, S.V.; Atala, A. 3D bioprinting of tissues and organs. *Nat. Biotechnol.* **2014**, *32*, 773–785. [[CrossRef](#)]
21. Decante, G.; Costa, J.B.; Silva-Correia, J.; Collins, M.N.; Reis, R.L.; Oliveira, J.M. Engineering bioinks for 3D bioprinting. *Biofabrication* **2021**, *13*, 032001. [[CrossRef](#)] [[PubMed](#)]
22. Selcan, G.O.P.; Inci, I.; Zhang, Y.S.; Khademhosseini, A.; Mehmet, R.D. Bioinks for 3D bioprinting: An overview. *Biomater. Sci.* **2018**, *6*, 915–946.
23. Lee, H.J.; Kim, Y.B.; Ahn, S.H.; Lee, J.S.; Jang, C.H.; Yoon, H.; Chun, W.; Kim, G.H. A New Approach for Fabricating Collagen/ECM-Based Bioinks Using Preosteoblasts and Human Adipose Stem Cells. *Adv. Health Mater.* **2015**, *24*, 1359–1368. [[CrossRef](#)] [[PubMed](#)]
24. Montanucci, P.; Basta, G.; Pescara, T.; Pennoni, I.; Di Giovanni, F.; Calafiore, R. New simple and rapid method for purification of mesenchymal stem cells from the human umbilical cord Wharton jelly. *Tissue Eng. Part A* **2011**, *17*, 2651–2661. [[CrossRef](#)] [[PubMed](#)]
25. Pittenger, M.F.; Mackay, A.M.; Beck, S.C.; Jaiswal, R.K.; Douglas, R.; Mosca, J.D.; Moorman, M.A.; Simonetti, D.W.; Craig, S.; Marshak, D.R. Multilineage potential of adult human mesenchymal stem cells. *Science* **1999**, *284*, 143–147. [[CrossRef](#)]
26. Jiang, J.; Au, M.; Lu, K.; Eshpeter, A.; Korbitt, G.; Fisk, G.; Majumdar, A.S. Generation of insulin-producing islet-like clusters from human embryonic stem cells. *Stem Cells* **2007**, *25*, 1940–1953. [[CrossRef](#)]
27. Ganta, C.; Chiyo, D.; Ayuzawa, R.; Rachakatla, R.; Pyle, M.; Andrews, G.; Weiss, M.; Tamura, M.; Troyer, D. Rat umbilical cord stem cells completely abolish rat mammary carcinomas with no evidence of metastasis or recurrence 100 days post-tumor cell inoculation. *Cancer Res.* **2009**, *69*, 1815–1820. [[CrossRef](#)]
28. Bartholomew, A.; Sturgeon, C.; Siatskas, M.; Ferrer, K.; McIntosh, K.; Patil, S.; Hardy, W.; Devine, S.; Ucker, D.; Deans, R.; et al. Mesenchymal stem cells suppress lymphocyte proliferation in vitro and prolong skin graft survival in vivo. *Exp. Hematol.* **2002**, *30*, 42–48. [[CrossRef](#)]
29. Di Nicola, M.; Carlo-Stella, C.; Magni, M.; Milanese, M.; Longoni, P.D.; Matteucci, P.; Grisanti, S.; Gianni, M.A. Human bone marrow stromal cells suppress T-lymphocyte proliferation induced by cellular or nonspecific mitogenic stimuli. *Blood* **2002**, *99*, 3838–3843. [[CrossRef](#)]
30. Alunno, A.; Montanucci, P.; Bistoni, O.; Basta, G.; Caterbi, S.; Pescara, T.; Pennoni, I.; Bini, V.; Bartoloni, E.; Gerli, R.; et al. In vitro immunomodulatory effects of microencapsulated umbilical cord Wharton jelly-derived mesenchymal stem cells in primary Sjögren's syndrome. *Rheumatology* **2015**, *54*, 163–168. [[CrossRef](#)]
31. Sato, K.; Ozaki, K.; Oh, I.; Meguro, A.; Hatanaka, K.; Nagai, T.; Muroi, K.; Ozawa, K. Nitric oxide plays a critical role in suppression of T-cell proliferation by mesenchymal stem cells. *Blood* **2007**, *109*, 228–234. [[CrossRef](#)]
32. Djouad, F.; Charbonnier, L.M.; Bouffi, C.; Louis-Pence, P.; Bony, C.; Apparailly, F.; Cantos, C.; Jorgensen, C.; Noel, D. Mesenchymal stem cells inhibit the differentiation of dendritic cells through an interleukin-6-dependent mechanism. *Stem Cells* **2007**, *25*, 2025–2032. [[CrossRef](#)]
33. English, K.; Barry, F.P.; Field-Corbett, C.P.; Mahon, B.P. IFN-gamma and TNF-alpha differentially regulate immunomodulation by murine mesenchymal stem cells. *Immunol. Lett.* **2007**, *110*, 91–100. [[CrossRef](#)]
34. Xu, G.; Zhang, L.; Ren, G.; Yuan, Z.; Zhang, Y.; Zhao, R.C.; Shi, Y. Immunosuppressive properties of cloned bone marrow mesenchymal stem cells. *Cell Res.* **2007**, *17*, 240–248. [[CrossRef](#)]

35. La Rocca, G.; Corrao, S.; Lo Iacono, M.; Corsello, T.; Farina, F.; Anzalone, R. Novel immunomodulatory markers expressed by humanWJ-MSC: An updated review in regenerative and reparative medicine. *Open Tissue Eng. Regen. Med. J.* **2012**, *5*, 50–58. [[CrossRef](#)]
36. Selmani, Z.; Naji, A.; Zidi, I.; Favier, B.; Gaiffe, E.; Obert, L.; Borg, C.; Saas, P.; Tiberghien, P.; Rouas-Freiss, N.; et al. Human leukocyte antigen-G5 secretion by human mesenchymal stem cells is required to suppress T lymphocyte and natural killer function and to induce CD4⁺ CD25^{high}FOXP3⁺ regulatory T cells. *Stem Cells* **2008**, *26*, 212–222. [[CrossRef](#)]
37. Montanucci, P.; Alunno, A.; Basta, G.; Bistoni, O.; Pescara, T.; Caterbi, S.; Pennoni, I.; Bini, V.; Gerli, R.; Calafiore, R. Restoration of t cell substes of patients with type 1 diabetes mellitus by microencapsulated human umbilical cord Wharton jelly-derived mesenchymal stem cells: An in vitro study. *Clin. Immunol.* **2016**, *163*, 34–41. [[CrossRef](#)] [[PubMed](#)]
38. Markstedt, K.; Mantas, A.; Tournier, I.; Ávila, M.H.; Hägg, D.; Gatenholm, P. 3D Bioprinting Human Chondrocytes with Nanocellulose-Alginate Bioink for Cartilage Tissue Engineering Applications. *Biomacromolecules* **2015**, *16*, 1489–1496. [[CrossRef](#)]
39. Basta, G.; Montanucci, P.; Calafiore, R. Microencapsulation of cells and molecular therapy of type 1 diabetes mellitus: The actual state and future perspectives between promise and progress. *J. Diabetes Investig.* **2021**, *12*, 301–309. [[CrossRef](#)]
40. Wang, J.H.; Thampatty, B.P. Mechanobiology of adult and stem cells. *Int. Rev. Cell Mol. Biol.* **2008**, *271*, 301–304.
41. Weiss, M.L.; Mitchell, K.E.; Hix, J.E.; Medicetty, S.; El-Zarkouny, S.Z.; Grieger, D.; Troyer, D.L. Transplantation of porcine umbilical cord matrix cells into the rat brain. *Exp. Neurol.* **2003**, *182*, 288–299. [[CrossRef](#)] [[PubMed](#)]

Disclaimer/Publisher’s Note: The statements, opinions and data contained in all publications are solely those of the individual author(s) and contributor(s) and not of MDPI and/or the editor(s). MDPI and/or the editor(s) disclaim responsibility for any injury to people or property resulting from any ideas, methods, instructions or products referred to in the content.